On the use of legacy AEM data

Viezzoli Andrea[1]*, Menghini Antonio[1] and Vlad Kaminski[1,2] discuss how time domain AEM data post-2000 can be most usefully used in the big data AI era.

Introduction

The term 'legacy data' is rather loose. It always means 'old data', but there is no consensus on what is 'old', especially across disciplines/data types. In this paper we focus on Time domain AEM data post 2000. By then, virtually all systems were equipped with a Digital Aquisition System (DAS). It is also around those years that Time Domain (TD) systems started to gain ground on Frequency Domain (FD) systems, thanks to the introduction of concentric helicopter borne systems. However, it is time domain systems that can most benefit from renewed analysis modelling. Time domain data can take longer to model, which is one of the reasons they were often never properly inverted at the time. On the other hand, they often span larger frequency ranges (3-4 decades instead of 2-3 of the FD) while also displaying clearer signatures of 'new' physical processes such as Airborne IP (AIP) and superparamagnetic effects (SPM). Finally, most development in new generation of AEM systems takes place in TD, which fosters continued R/D.

There are several good reasons to give another look at 'legacy' AEM data.

First of all, the largest part of the investment (i.e., data aquisition) has already been undertaken; secondly, the datasets are often very sub-utilized; thirdly, as mentioned above, there is strong Research and Development that is enabling us to understand phenomena which were previously flagged as noise, or disregarded; fourthly, we witness the push for integrating data from different sources; last, but not least, the huge amount of spatial data associated with AEM represent a formidable attraction to big data-AI.

Here we touch briefly on two aspects of the benefits of reinspecting legacy AEM data: general geological mapping and modelling IP effects.

Geological mapping/merging dataset

Very often, especially in high greenfield exploration, AEM data were aquired and then analysed with a bump-finding approach. Targets of interest for follow up would usually be areas with local increase of signal at late times, with the hope they would represent 'bedrock conductors'. Like for any measurement of physical properties, the measured AEM data depends on the specification of instrument used to carry out the measurement (in technical terms, on its transfer function). This means that the same conductor will give different readings when measured with system A or system B, or even by system A, at given heights. Even if the analysis did not stop at the mere data-space and the data were 'modelled', such modelling would usually involve fast transforms that yield 'imaging', the likes of Emflow's Conductivity Depth Imaging (CDI) or of Geotech's (REF) Conductivity Depth Imaging (RDI). This approach is typical of, although not limited to, junior miners. It is also often followed in government-sponsored regional mapping aimed at incentivizing exploration. These imaging techniques are extremely fast and provide a fair first glance into the model space, but are far from the accuracy of the results produced by more advanced modelling such as full non-linear inversions and/or plate modelling. The net result of such an approach is that a) the results obtained are way less accurate and trustworhty than they could be, b) the vast majority of the information about subsurface present in the data was overlooked. These datasets can therefore be reprocessed and remodelled to extract it, obtaining a geological model of the area. This can bring huge added value to different stages of the exploration programme. For example, specific geological units can be crucial to potential development of mineralization. Also knowing depth to bedrock is always relevant. In either case, obtaining robust geological information from the AEM proves useful for the continuation of exploration, for example by reducing the search space for ground follow-up, better designing ground geophysical campaigns and allowing more stringent integration with ancillary data.

Of particular relevance is the situation where several AEM surveys have been carried out in a given area, by different contractors, over a period of time. In these cases, the individual surveys would have usually been looked at independently, either as voltage at given times, or as CDIs. Given that none of these two approaches take the transfer function of the AEM systems out of the equation, bringing these independent products together most often results in obvious artefacts at the edges of the surveys. Merging them into a single frame of coherent, seamless maps/models requires full non-linear inversions with accurate forward modelling that fully describe the different specs of each of the AEM systems.

Beside this general call for extracting geological information from the AEM data, there is a special case in which remodelling legacy data provides even more striking results: IP effects in AEM data.

AIP

Let us start with some important semantics to explain the difference bewteen ground and Airborne IP. What is usually

[1]Aarhus Geophysics Aps, Denmark | [2]Promisedland Exploration, Canada
* Corresponding author, E-mail: andrea.viezzoli@aarhusgeo.com

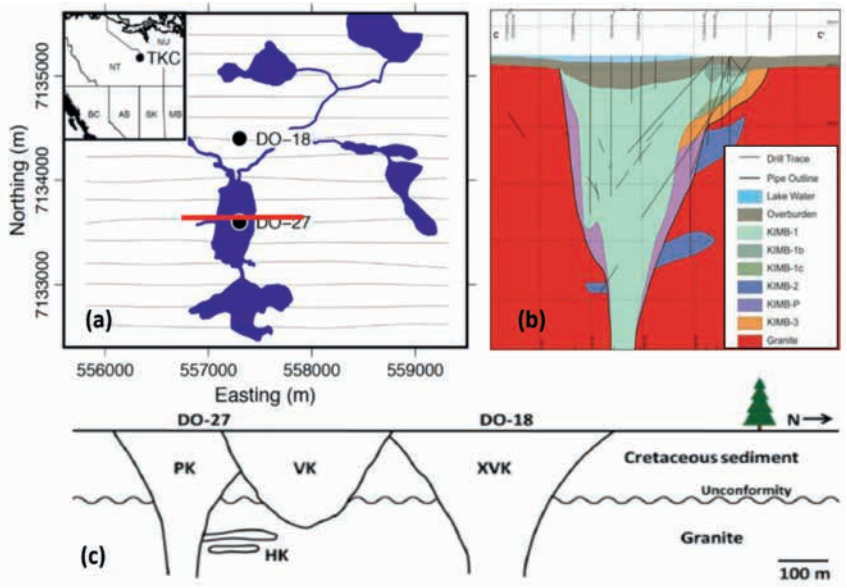

Figure 1 a) Location of Tli Kwi Cho kimberlite complex in northern Canada. b) Structure of DO-27 kimberlite pipe. (adapted from Harder et al., 2008). c) Schematic geological cross-section drawn in a N–S direction across the two kimberlite pipes of Tli Kwi Cho complex (adapted from Devriese et al., 2014).

referred to as Induced Polarization is the dispersive nature of resistivity (conductivity) at frequencies typical of ground IP surveys. Such fundamental phenomenon is then translated into different parameters such as chargeability, metal factor, and phase lag, depending mainly on the domain (time versus frequency) and equipment used. It is at these frequencies that many discoveries have been made. The dispersivity of resistivity, however, takes place also at higher frequencies, including those of the AEM systems. Such phenomenon can only therefore still be explained with the polarization of the subsurface, hence the name AIP (airborne IP). The unmistakable signature of IP effects in central TDEM systems is the opposite polarity of the transient, or parts thereof. IP effects in AEM data have long been known (REF). However, for decades, the industry lacked interest in and widespread understanding of the physics behind them, and reliable codes to model them. As a result, they were discarded, avoided, at times hidden, most often mistaken for other sources of 'noise'. It was only a few years ago that the conditions ripened for an overall review of AIP, its meaning and relevance for exploration and other applications. Bigger AEM systems, displaying lower base frequency, better S/N, sounder post-processing procedures, and new modelling codes have all helped to turn AIP into a true, widely accepted phenomenon that the industry must come to terms with. Recent research shows how AIP can, for example in presence of certian type of geological sequences, produce surprising signatures in the transients, extending beyond the classical single sign reversal. Perhaps the biggest selling point for AIP is that, even if one did not care at all about chargeability, once the AEM data is affected by IP, if the latter is not modelled correctly, the resistivities (conductivities) will be severely affected by artefacts. This effects extend to the very bottom of the resistivity models, making AIP something relevant to great depths. Those that do care about chargeability should be clear that AIP does not provide exactly the same information as ground IP (nor as IP measured in the lab), due to the different frequency range they operate at. At times, when the spectra overlap, there can be similarities. At other times they can provide complementary information about, e.g, alterations in the proximity of the mineralization. Latest research also shows that, under certain conditions, chargeability can be recovered from AEM to depths in excess of 200 m.

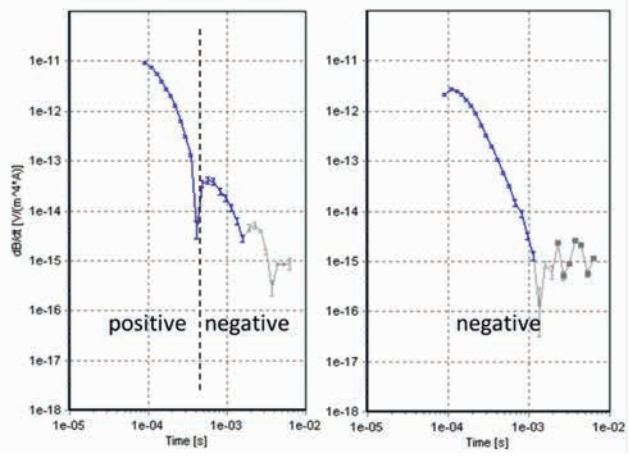

Figure 2 Transient centred over DO27 (left) and DO 18 (right), showing polarities.

TliKwiCho

A typical example of revisting AEM data affected by IP effects is given by the Tli Kwi Cho kimberlites project. Tli Kwi Cho is a kimberlite complex, located within the Lac de Gras area of Archaean Slave Craton in the North West Territories, Canada. It was discovered in 1992 during drill-sampling of paired geophysical anomalies DO-18 and DO-27. Core drilling revealed four major rock types (Doyle et al., 1998), including HK (hypabyssal facies), PK (pyroclastic facies), VK (volcaniclastic facies) and XVK (xenolith-rich volcaniclastic facies).

The complex is situated approximately 350 km northeast of Yellowknife, NWT, Canada and consists of two pipe-like kimberlitic bodies (DO-18 and DO-27). One of the pipes (DO-27) is situated predominantly underneath lake waters (Figure 1a). The kimberlitic complex is hosted within the granites, granodiorites and gneisses of Yellowknife supergroup (Kjarsgaard et al., 2002). The structure of kimberlite pipe DO-27 is shown in Figure 1b, while Figure 1c shows a schematic geological cross-section with

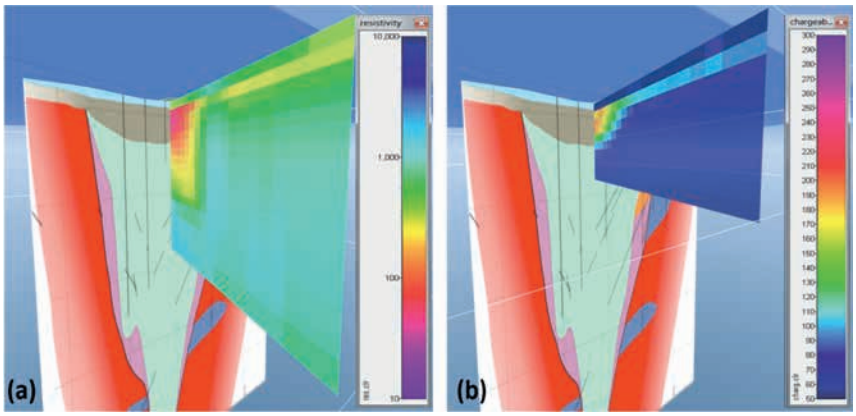

Figure 3 a) Interpolated electrical resistivity recovered from IP-mode SCI inversion of VTEM data flown over DO-27 kimberlite. b) Interpolated chargeability recovered from IP-mode SCI inversion of VTEM data flown over DO-27 kimberlite.

different facies of kimberlite marked as following: PK: green pyroclastic facies; VK: black volcaniclastic facies and HK: grey hypabyssal facies.

In Figure 1b, the diversity of kimberlitic facies is greater, than in Figure 1c. In particular, the pyroclastic facies (PK) has been substratified into three units (KIMB-1, KIMB-1b and KIMB-1c); the volcaniclastic facies (VK) has been substratified into two units (KIMB-P and KIMB-3), while KIMB-2 represents intrusive coherent sheets, a unit not present in Figure 12c.

Multiple geophysical surveys have been conducted over the prospect since early 1990s, including a VTEM survey, which was flown in 2004. Some of the recorded voltage values over the kimberlites are negative, which indicates presence of chargeable material. This is referred to as airborne IP effect (AIP effect) and has been previously described in the literature (Smith and Klein, 1996). Such effects have been recorded over other kimberlites in ground TDEM data (Kamenetsky et al., 2014) and in airborne data (Kaminski and Viezzoli, 2017).

Methodology for AIP modelling

Transients recorded over DO-18 are mainly negative, while transients recorded over DO-27 show both positive and negative voltages (cfr Figure 2).

The VTEM data set reprocessed from scratch, using Aarhus Workbench (Aarhus Geosoftware). This entailed mainly assessing noise levels, which may vary across the survey. All gates above noise negatives were kept, regardless of their polarity. Editing out the noise can be especially complicated in presence of IP, due to the low signal levels, and the potential ambiguity of some features. The data were inverted using the Spatially Constrained Inversion approach (SCI, Viezzoli et al., 2008), modified as per Fiandaca et al. (2012) in order to accommodate modelling of parameters of the famous Cole Cole model. The latter has been widely and successfully used in exploration with ground IP. It comprises four parameters: r(0), m, c and t, respectively the dc resistivity, chargeability, frequency component and time constant. The high frequencies of the AEM systems excite mainly low time constants.

Solving for three extra parameters increases non-uniqueness and requires extra attention to inversion strategies, with regularization playing a major role. The SCI approach is instrumental in reducing ambiguity, limiting the spatial covariance of model parameters. Importantly, dozens of preliminary inversions with different starting parameters are carried out in order to thoroughly explore the model space. No a-priori information were applied to the inversions.

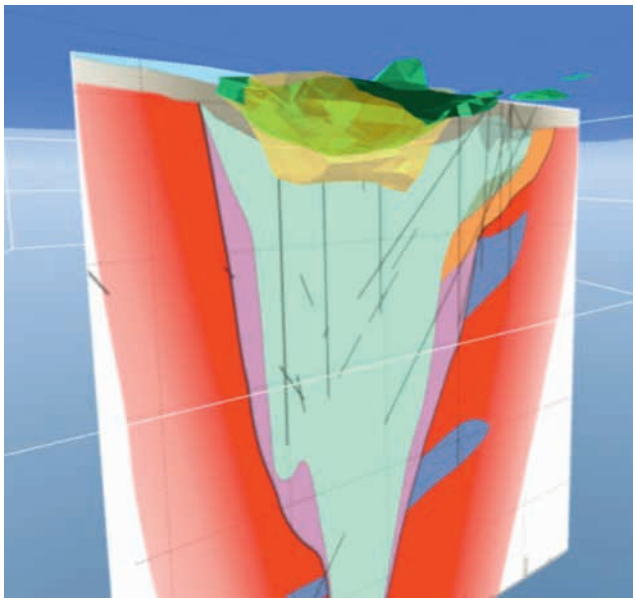

Figure 4 Iso volumes of resistivity (200 ohmm) and chargeability (120 mV/V).

Like for any other type of modelling, data processing is a recursive exercise, where preliminary results are carefully analysed against ancillary information. In presence of possible artefacts that can be ascribed to incorrect processing, the data undergoes another round of (post)processing.

The final results of the SCI inversion were imported in GeoScene3D (I-GIS) and verified against the lithological cross-sections. In Figure 3a an interpolated resistivity section is shown over DO-27 kimberlite, while the recovered chargeability is shown in Figure 3b.

Further conductivity and chargeability shells were constructed (Figure 4) in order to contour areas with inverted resistivities smaller than 200 Ohm m and inverted chargeabilities smaller than 120 mV/V.

Cole-Cole parameters recovered in the SCI inversion attempt were compared (Figure 5) against the Cole-Cole parameters estimated from rock samples in GSC lab (Oldenburg and Kang, 2016). The overall agreement is very satisfactory, especially taking into account the different sampling volumes and measurement frequencies.

Further to the inversion of VTEM data in IP mode, the corresponding Total Magnetic Intensity (TMI) data set was inverted using mag3D software (Li and Oldenburg, 1996). The inversion was carried out over a 10m x 10m by 5m mesh with voxel thickness gradually increasing to 100 m. Standard deviation was set to 3nT and the inversion has converged in four iteration steps. As a result, a 3D magnetic susceptibility model was recovered (Figure 6).

The recovered physical properties were further classified on to a common 3D mesh (cfr Kaminski et al., 2017), using a-priori information with the following assumptions, as shown in Table 1.

The resulting 3D pseudo-lithological distribution was compared to lithology derived from drilling and is shown in Figure 7.

The depth of investigation and resolution are different for the SCI inversion results and mag3D inversion results, which has to be taken into the account, when all recovered physical properties

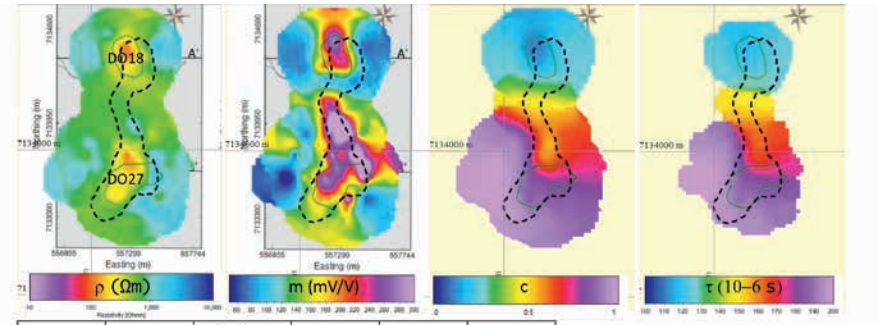

	division	ρ(∞) (Ωm)	m (mV/V)	τ(μs)	c
DO18	XYK	81	540	40	0.6
DO27	VK	49	340	100	0.7

Figure 5 Comparison of Cole-Cole parameters estimated from rock samples at GSC lab (adapted from Oldenburg and Kang, 2016) vs Cole-Cole parameters recovered from VTEM data.

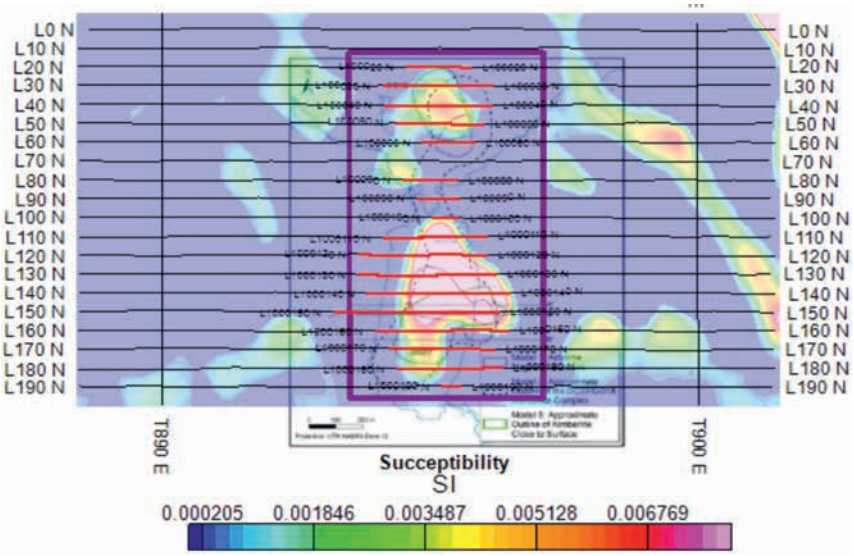

Figure 6 Recovered magnetic susceptibility at abs. elevation level of 311 m.

Classes	Resistivity (Ohm m)	Magnetic susceptibility (*10-5 SI)	Chargeability (mV/V)	Depth (m)	Remarks
Lake water	500 to 1300	-	< 75	<30	Lake over DO-27
Overburden	< 500	-	> 75	<50	
Granodiorites	> 1300	< 600	-	-	
Kimberlite facies					
VK	-	600 to 2000	-	-	Volcaniclastic
PK	-	600 to 2000	-	-	Pyroclastic
HK	-	> 2000	-	-	Hypabissal
XVK	-	600 to 2000	-	-	Volcaniclastic (DO-18)

Table 1 A-priori information and other assumptions used in defining different classes for pseudo-lithological 3D distribution, based on recovered physical properties.

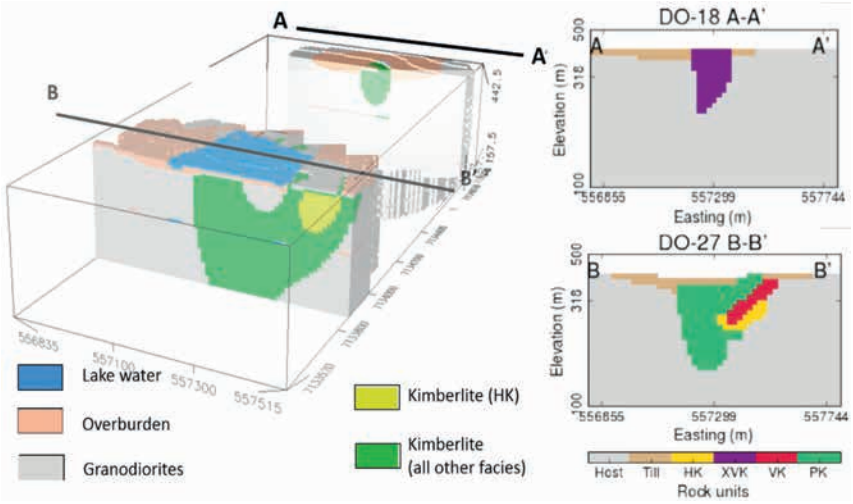

Figure 7 Comparison of pseudo-lithology derived from inversions of geophysical data (left) with the lithotypes, derived from drilling (right, Devriese et al., 2017).

are matched together in a classification attempt, therefore the chargeability and resistivity are only used in the classification of the topmost strata.

Analysing the inversion results it becomes conclusive that the inversion in IP mode of the VTEM data is imaging the upper part of kimberlite and the clay-rich overburden as electrically conductive (< 200 Ohm m), while the chargeable material is limited to the clay-rich overburden. The conductive upper part of the kimberlite may be due to a high degree of fractures. Overall the inversion was successful in modelling the VTEM data with IP effect and recovering the Cole-Cole parameters from the data. The magnetic inversion is helpful in delineating all the kimberlitic facies from granodioritic host rock and furthermore can be used to separate hypabyssal facies (highest magnetic susceptibility) from other facies. Overall, the suggested methodology is successful in delineating 3D pseudolithology, when compared to lithologies, derived from drilling. This rock type classification methodology based on user-defined clustering is seen as potentially viable at advanced exploration stages and increasingly attractive with greater availability of ancillary data. We refer to Fournier et al. (2017) and Devriese et al. (2017) for an overview of complementary modelling of the same dataset.

Conclusions

AEM legacy data have a lot to offer, to either exploration or hydrogeological mapping, or general geological modelling. A significant amount of extra, quantitative information can be extracted from them, thanks to modern processing procedures, better understanding of the physics and more advanced modelling codes.

Acknowledgments

The authors would like to thank Ken Witherly for organizing the 2016 SEG workshop shoot-out from which the TKC results largely originate.

References

Aarhus Geosoftware [2019]. https://www.aarhusgeosoftware.dk/

Devriese, S.G.R., K. Davis, and D.W. Oldenburg [2017]. Inversion of airborne geophysics over the DO-27/DO-18 kimberlites - Part 1: Potential fields. *Interpretation*, **5**, T299-T311.

Doyle, B., Kivi, K., Scott Sith, B.H. [1998]. The Tli Kwi Cho (DO27 and DO18) diamondiferous kimberlite complex, Slave craton, NWT, Canada. *VII International kimberlite Conference*, Abstracts.

Fournier, D., S. Kang, M.S. McMillan, and D.W. Oldenburg [2017]. Inversion of airborne geophysics over the DO-27/DO-18 kimberlites - Part 2: Electromagnetics. *Interpretation*, **5**, T313-325.

I-GIS [2019]. http://i-gis.dk/da-dk/

Kang, S., D. Fournier, and D.W. Oldenburg [2017]. Inversion of airborne geophysics over the DO-27/DO-18 kimberlites - Part 3: Induced polarization. *Interpretation*, **5**, T327-340.

Kamenetsky, F., Trigubovich, G. and Chernyshev, A. [2014]. *Three lectures on geological medium induced polarization*. Ludwig-Maximilian University of Munich.

Kaminski, V. and Viezzoli, A. [2017]. Modeling induced polarization effects in helicopter time-domain electromagnetic data: Field case studies. **82**(2), *Geophysics,* B49-B61.

Kaminski, V., Viezzoli, A., Paasche, H. and Manca, G. [2017]. Three dimentional pseudolithology derived from inversions of airborne geophysical data, *EAGE Near Surface Geoscience*, Extended Abstracts.

Macnae, J. [2016]. Quantitative estimation of intrinsic polarization and superparamagnetic parameters from airborne electromagnetic data. *Geophysics* **81**(6), E433-E446.

Oldenburg, D. and Kang., S. [2016]. Airborne IP for Kimberlite. *4th international workshop on induced polarization,* Abstracts.

Smith, R.S. [1989]. On induced polarization effects in time domain electromagnetic measurements, discussion, *Geophysics*, **54**, 514-523.

Viezzoli, A., Kaminski, V. and Fiandaca, G. [2017]. Modeling induced polarization effects in helicopter TEM data: Synthetic case studies. *Geophysics*, **82**(2) E31-E50.